

PHASE STABILITY AND SEMICONDUCTING BEHAVIOUR OF LOW ACTIVATION AUSTENITIC MN-CR STEELS

A. Fattah-alhosseini¹, *and M. Asadi Asadabad²

* a.fattah@basu.ac.ir

Received: March 2014

Accepted: October 2014

¹ Faculty of Engineering, Bu-Ali Sina University, Hamedan, Iran.

² Materials Research School, Nuclear Science and Technology Research Institute, Isfahan, Iran.

Abstract: Four compositions of austenitic Mn-Cr steels have been developed successfully for in-vessel component materials in power plant industry. The phase stability of these Mn-Cr steels was studied by and X-ray diffraction (XRD) patterns. XRD patterns have shown that the matrix of these Mn-Cr steels is a single γ -phase structure. The potentiodynamic polarisation curves suggested that these fabricated Mn-Cr steels showed passive behaviour in 0.1M H_2SO_4 solution. Therefore, semiconducting behaviour of passive film formed on these fabricated Mn-Cr steels in 0.1M H_2SO_4 solution was evaluated by Mott-Schottky analysis. This analysis revealed that passive films behave as n-type and p-type semiconductors. Based on the Mott-Schottky analysis, it was also shown that donor and acceptor densities are in the order of 10^{21} cm^{-3} and are comparable for other austenitic stainless steels in acidic environments.

Keywords: Low activation; Mn-Cr steel; XRD; Mott-Schottky.

1. INTRODUCTION

Low activation austenitic Mn-Cr steels are candidate materials for structural components of power plant industry [1-3]. These steels are possible alternatives to Fe-Cr-Ni-based austenitic steels, on the basis of substitution of the strategic element Ni by the more plentiful and cheaper metal Mn [4-6].

Other main advantages of Mn-Cr steels can be found in their applications in wear-resistant and pitting-resistant steel products. These steels have also been successfully applied in the superconductor industries. This is mainly because of their higher strengths in cryogenic environments [7-9].

Various types of low activation austenitic steels have been developed based on Mn-Cr non-magnetic steels [10-12]. It has reported [13, 14] that the phase and properties of Mn-Cr steels are unstable under irradiation at high temperature. Although the applicability of the steels to fusion reactor components may be limited due to such characteristics, further investigation has been conducted to optimize their properties and minimize the effects of radiation damage. Shamardin et al. [15] have investigated various types of low activation austenitic stainless steel based on Mn-Cr non-magnetic steels. However, those alloys still have

small amounts of Ni, Co, Mo, etc. which cause problems of long-life activation.

In the present study, research has been conducted firstly to eliminate such undesirable elements and produce lower activation austenitic Mn-Cr steels that can be manufactured along usual industrial production lines. Also, low activation austenitic Mn-Cr steels frequently come in contact with acids during the process like cleaning, and pickling. Therefore, studying the corrosion behaviour of these steels in the acidic solution is of prime importance. Therefore, this research has also been focused on the semiconducting behaviour of Low activation austenitic Mn-Cr steels in 0.1M H_2SO_4 solution.

2. EXPERIMENTAL PROCEDURES

Four austenitic Mn-Cr steels listed in Table 1 were fabricated by a vacuum high-frequency induction furnace which was used to cast a single ingot for each steels.

To prepare sheets from these steels, hot rolling was carried out on 40 mm thick ingots. Initially the steels were heated to 1200 °C for 120 min. the thickness was reduced to 30 and then 22 mm. Afterwards the sheets were heated to 1100 °C for 10 min and a further reduction to 18 and finally 10 mm was applied on the sheets. In order to achieve a

Table 1. Chemical compositions of four fabricated austenitic Mn-Cr steels.

	C	Cr	Mn	V	Si	P	S	Fe
Mn-Cr Steel 1	0.126	10.21	23.58	0.068	0.103	0.005	0.008	Bal.
Mn-Cr Steel 2	0.065	12.51	23.12	0.095	0.056	0.005	0.011	Bal.
Mn-Cr Steel 3	0.277	12.01	19.58	0.055	0.176	0.006	0.011	Bal.
Mn-Cr Steel 4	0.141	12.55	23.41	0.073	0.132	0.006	0.009	Bal.

homogenous structure annealing was carried out at 1050°C for 10 minutes and the sheets were quenched in water [16]. XRD was used for phase evaluations using Philips PW-1800, Cu K α .

For electrochemical measurements, test samples were cut from the plates and polished mechanically by abrading with wet emery paper up to 2000 grit size on all sides and then were embedded in cold curing epoxy resin. Prior to all measurements, working electrodes were degreased with acetone, rinsed with distilled water and dried with a stream of air.

Electrochemical measurements were performed in a conventional three-electrode cell under aerated conditions. The counter electrode was a Pt plate, while the reference electrode was Ag/AgCl saturated in KCl. Electrochemical measurements were obtained by using a Autolab potentiostat/galvanostat system. Prior to all electrochemical measurements, working electrodes immersed at open circuit potential (OCP) for 0.5 h to form a steady-state passive film.

Potentiodynamic polarization curves were measured potentiodynamically at a scan rate of 1

mV/s starting from $-0.25 V_{Ag/AgCl}$ (vs. E_{corr}) to $2.0 V_{Ag/AgCl}$. Mott-Schottky analysis were carried out on passive films at a frequency of 1 kHz using a 10 mV ac signal, and a step rate of 25 mV in the cathodic direction.

3. RESULTS AND DISCUSSION

3. 1. Development of Low Activation Austenitic Mn-Cr Steels

Mn is an important element to stabilize the austenite structure. However, an excess amount of Mn accelerates the production of intermetallic compounds and lowers ductility and corrosion resistance. Therefore, Mn was limited between 15% and 35%. Otherwise, a Cr content of more than 11% improves corrosion resistance. On the other hand, an excess amount of Cr destabilizes the austenite structure; therefore, the Cr content was limited in the range of 11% to 20%. Si is an effective deoxidizing element. An excess amount of Si, however, leads to the destabilization of the

Table 2. The calculated Cr and Ni equivalents for four fabricated Mn-Cr steels.

	Cr Equivalent, wt%	Ni Equivalent, wt%
Mn-Cr steel 1	10.76	15.58
Mn-Cr steel 2	13.09	13.51
Mn-Cr steel 3	12.63	17.90
Mn-Cr steel 4	13.22	15.93

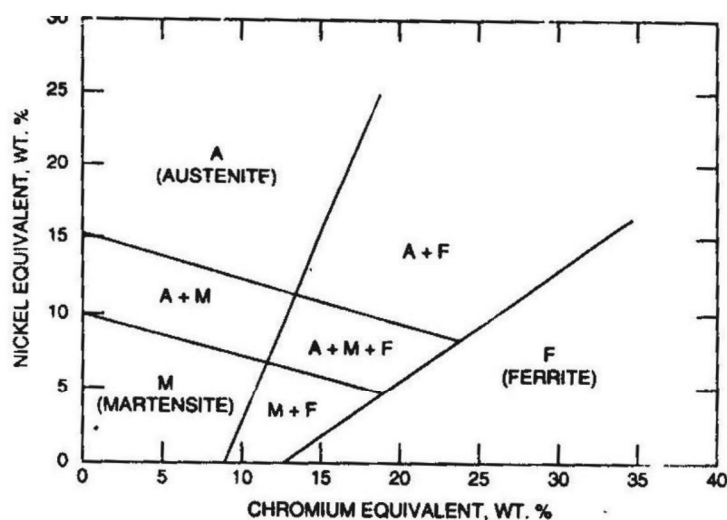


Fig.1. The corrected Schaeffler diagram for steels containing high amounts of Mn and Cr (maximum 40 wt.% Mn) [17].

austenite structure. So, the Si content was limited to 1.0% reduction of strength caused by the decreased amounts of C and N can be compensated for by adding V, which is intended to precipitate carbide and/or nitride. However, since an excess of V reduces weldability, V was restricted to 0.3%. Adjustment of alloying elements was conducted to obtain a single austenitic phase according to the constitution of austenitic stainless steels, which was based on the constitution diagrams of Schaeffler. Development of the Mn-Cr based stainless steels was done by considering the above factors [16].

The Schaeffler diagram is one of the means of determining the stability of austenite and other phases in the matrix of stainless steels. For the Schaeffler diagram, the nickel and chromium equivalents were calculated according to the following relationships [17, 18]:

$$\text{Nie} = (\text{Ni}) + (\text{Co}) + 0.5 (\text{Mn}) + 0.3 (\text{Cu}) + 25 (\text{N}) + 30 (\text{C}) \quad (1)$$

$$\text{Cre} = (\text{Cr}) + 2 (\text{Si}) + 1.5 (\text{Mo}) + 5 (\text{V}) + 5.5 (\text{Al}) + 1.75 (\text{Nb}) + 1.5 (\text{Ti}) + 0.75 (\text{W}) \quad (2)$$

where the concentrations of the respective elements given in parentheses are in weight percent. Klueh et al. [17] illustrated that Schaeffler diagram is not able to predict the amount of phases in steels containing high

amounts of Mn and needs some corrections. This led to a new Schaeffler diagram for steels containing high amounts of Cr and Mn (maximum 40 wt.% Mn) as is shown in Fig. 1.

Table 2 shows the calculated Chromium and Nickel equivalents using relations 1 and 2 for four types of austenitic Mn-Cr steels. It is apparent that using corrected Schaeffler diagram, the matrix of these Mn-Cr steels is single phase austenite. Fig. 2 shows the X-ray diffraction patterns of four types of austenitic Mn-Cr steels which show the XRD patterns of single austenite peak.

3. 2. Corrosion Behaviour

In Fig. 3, changes on OCP of four austenitic Mn-Cr steels in 0.1M H₂SO₄ solution is shown. At the start of immersion a reduction of the potential in four austenitic Mn-Cr steels immediately show the dissolution of oxide layer of the surface in an acidic environment. However, as time passes, the open circuit potentials tend towards positive amount. This trend is also reported for austenitic stainless steels in an acidic environment [19] which is indicative of the formation of growing layer and its role in increasing protectivity with time. Fig. 3 also indicates that after 1800 s a complete stable condition is achieved and electrochemical tests

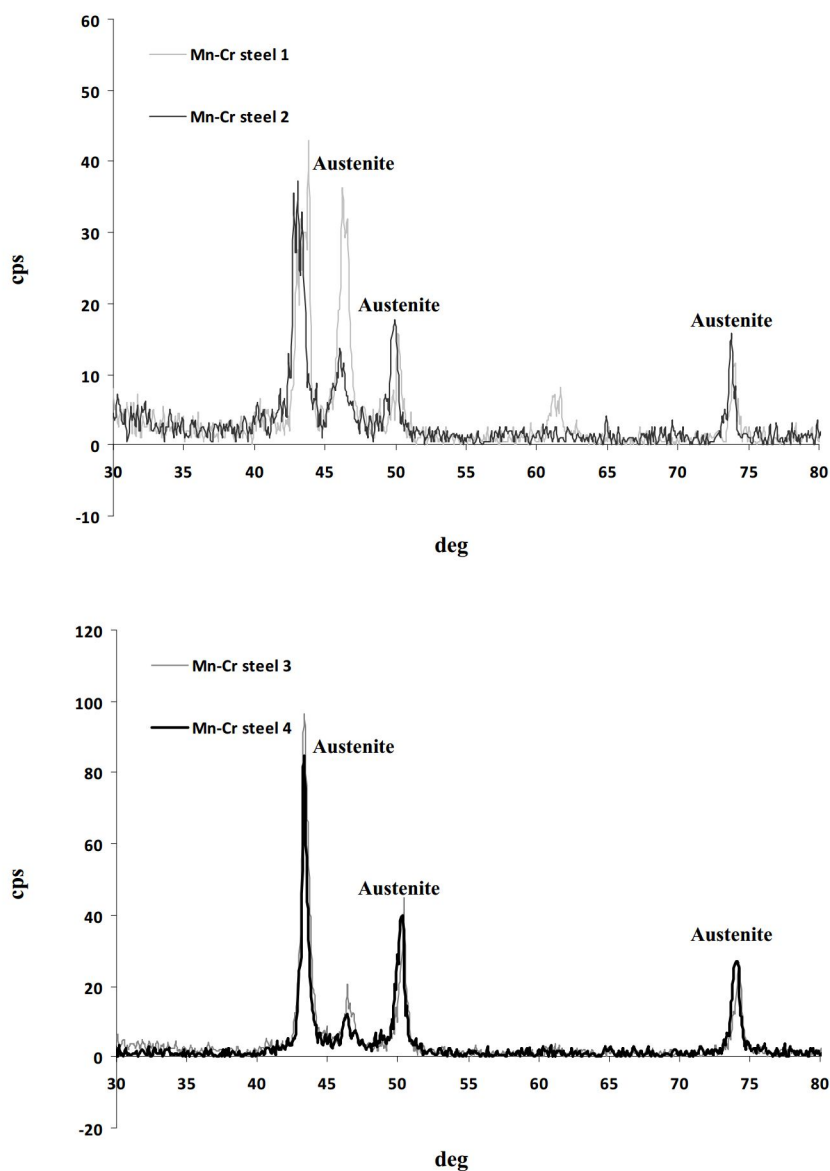


Fig. 2. XRD patterns of four fabricated Mn-Cr steels.

are possible.

Fig. 4 shows the potentiodynamic polarization curves of four austenitic Mn-Cr steels in 0.1M H₂SO₄ solution. For four curves, it is observed that before the electrode surface is transferred to a passive state an active current peak occurs, which could be related to the oxidation of Fe²⁺ to Fe³⁺ ions in the passive film [20, 21].

3. 3. Mott-Schottky Analysis

The outer layer of passive films contains the

space charge layer and sustains a potential drop across the film. The charge distribution at the semiconductor/solution is usually determined based on Mott-Schottky relationship by measuring electrode capacitance C, as a function of electrode potential (E) [22-25]:

$$\frac{1}{C^2} = \frac{2}{\epsilon\epsilon_0 e N_D} \left(E - E_{FB} - \frac{kT}{e} \right)$$

for n-type semiconductor (3)

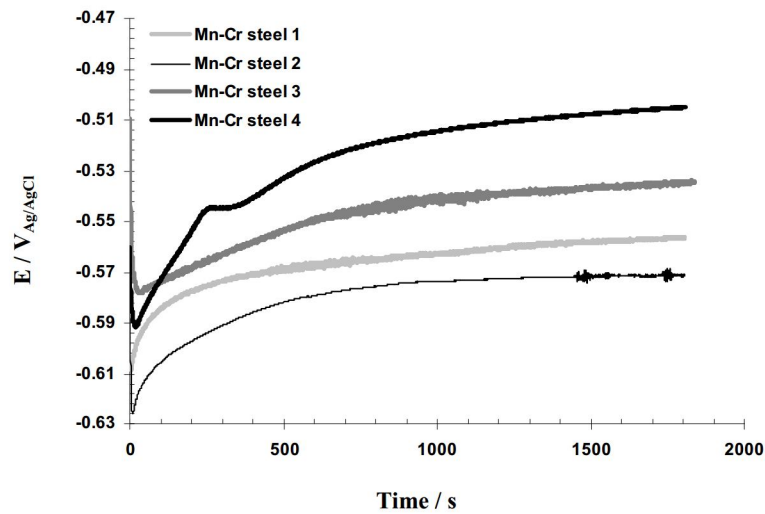


Fig.3. OCP plots of four fabricated Mn-Cr steels in 0.1M H₂SO₄ solution.

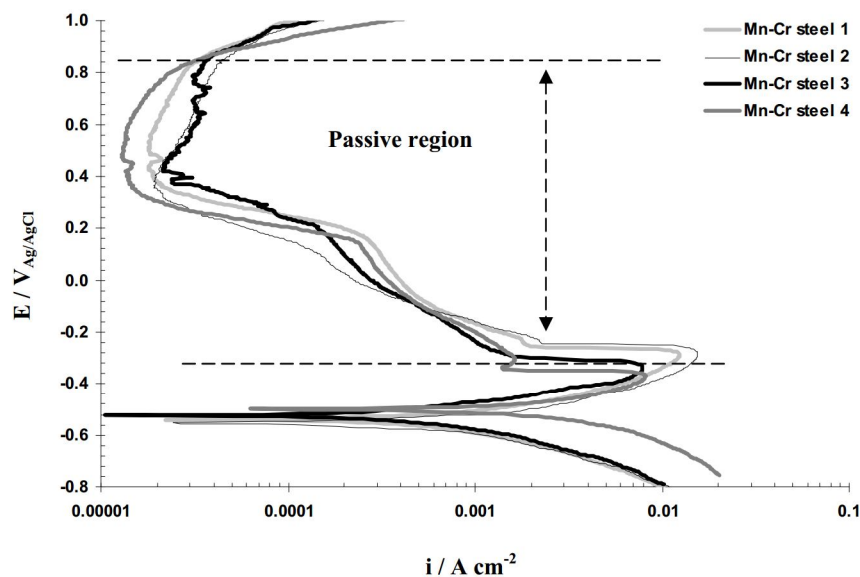


Fig.4. Potentiodynamic polarization plots of four fabricated Mn-Cr steels in 0.1M H₂SO₄ solution.

$$\frac{1}{C^2} = -\frac{2}{\epsilon\epsilon_0 e N_A} \left(E - E_{FB} - \frac{kT}{e} \right)$$

for p-type semiconductor (4)

where e is the electron charge (-1.602×10^{-19} C), N_D is the donor density for n-type semiconductor (cm^{-3}), N_A is the acceptor density

for p-type semiconductor (cm^{-3}), ϵ is the dielectric constant of the passive film (usually taken as 15.6), ϵ_0 is the vacuum permittivity (8.854×10^{-14} F cm^{-1}), k is the Boltzmann constant (1.38×10^{-23} J K^{-1}), T is the absolute temperature and E_{FB} is the flat band potential [22-25].

Fig. 5 shows the Mott-Schottky plots of four austenitic Mn-Cr steels in 0.1M H₂SO₄ solution.

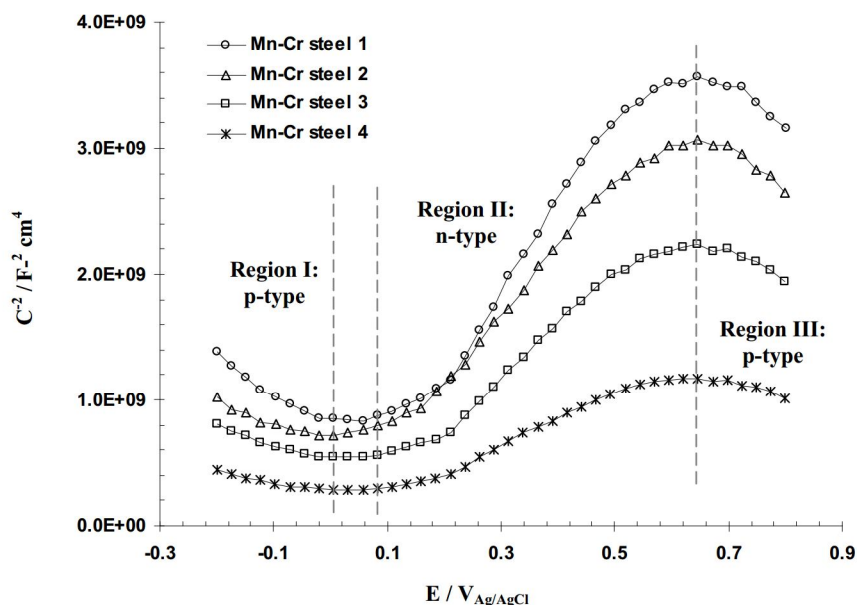


Fig.5. Mott-Schottky plots of four fabricated Mn-Cr steels in 0.1M H₂SO₄ solution.

Clearly, all plots show three regions in which a linear relationship between C^{-2} and E could be observed from them. The negative slopes in regions I and III are attributed to p-type behaviour. Region II presents positive slope, which depicts an n-type semiconducting behaviour.

Fig. 5 shows the passive films formed on these Mn-Cr steels behave as n-type and p-type semiconductors. This behaviour implies that the passive films have a duplex structure. Early studies of the bipolar duplex structures of passive films on stainless steels was done by Sato [26],

and followed by other researchers [27, 28]. It has been well established that the inner part of the passive film, which has a p-type behaviour, consists mainly of Cr oxides, while the outer region, with an n-type behaviour, predominantly consists of Fe oxides [29].

According to Eq. (3) and (4), donor and acceptor densities are determined by positive and negative slopes in regions II and III. Table 3 shows the calculated donor and acceptor densities for four austenitic Mn-Cr steels in 0.1M H₂SO₄ solution. The orders of magnitude are about 10^{21} cm⁻³ and are comparable for other austenitic

Table 3. Calculated donor and acceptor densities of the passive films formed on four fabricated Mn-Cr steels in 0.1M H₂SO₄ solution.

	Donor densities, cm ⁻³	Acceptor densities, cm ⁻³
Mn-Cr steel 1	1.271×10^{21}	2.041×10^{21}
Mn-Cr steel 2	1.618×10^{21}	2.313×10^{21}
Mn-Cr steel 3	2.056×10^{21}	3.648×10^{21}
Mn-Cr steel 4	3.961×10^{21}	6.933×10^{21}

stainless steels in acidic environments [30-32].

Changes in donor and acceptor densities correspond to the non-stoichiometry defects in passive films. Therefore, it can be concluded that the passive film on four austenitic Mn-Cr steels is disordered. Based on the Point Defect Model (PDM) [29], the donors or acceptors in semiconducting passive layers are point defects. The PDM postulates that the point defects present in a passive film are cation vacancies, oxygen vacancies, and cation interstitials. Cation vacancies are electron acceptors, thereby doping the barrier layer p-type, whereas oxygen vacancies and metal interstitials are electron donors, resulting in n-type doping.

For pure metals, the passive film is essentially a highly doped, defect semiconductor, as demonstrated by Mott-Schottky analysis. Not unexpectedly, the situation with regard to alloys is more complicated than for pure metals; because substitution of other metal cations, having oxidation states different from the host, on the cation sublattice may also impact the electronic defect structure in the film.

4. CONCLUSIONS

The phase stability and semiconducting behaviour of four austenitic Mn-Cr steels in 0.1M H₂SO₄ solution were investigated in the present work. Conclusions drawn from the study are as follows:

1. The amounts of nickel and chromium equivalents and also corrected Schaeffler diagram show that the microstructures of four Mn-Cr steels are only austenite. This is also confirmed by XRD evaluations.
2. The potentiodynamic polarization curves show that four fabricated Mn-Cr steels showed excellent passive behaviour in 0.1M H₂SO₄ solution
3. Mott-Schottky analysis showed existence of a duplex passive film structure composed of four oxide layers of distinct semiconductivities (n-type and p-type).
4. Also based on the Mott-Schottky analysis, it was shown that donor and acceptor densities are in the order of 10²¹ cm⁻³ and

are comparable for other austenitic stainless steels in acidic environments.

REFERENCES

1. Lula, R. A., "In Manganese Stainless Steels". The Manganese Centre, Paris, 1986, p. 1.
2. Kemp, M., Van Bennekom, A., and Robinson, F. P. A., "Evaluation of the corrosion and mechanical properties of a range of experimental Cr-Mn stainless steels", Mater. Sci. Eng. A, 1995, 199, 183.
3. Nijhawan, B. R., in Stainless Steels '87. The Institute of Metals, York, 1987, p. 535.
4. Bi, H. Y., Jiang, X. X., and Li, S. Z., "The corrosive wear behavior of Cr-Mn-N series casting stainless steel", Wear, 1999, 225, 1043.
5. Chen, S. R., Davies, H. A., and Rainforth, W. M., "Austenite phase formation in rapidly solidified Fe-Cr-Mn-C Steels", Acta mater., 1999, 47, 4555.
6. Zhang, Y. S., Zhu, X. M., and Zhong, S. H., "Effect of alloying elements on the electrochemical polarization behavior and passive film of Fe-Mn base alloys in various aqueous solutions", Corros. Sci., 2004, 46, 853.
7. Lenel, U. R., and Knott, B. R., "Structure and properties of corrosion and wear resistant Cr-Mn-N steels", Metall. Trans., 1987, 18A, 847.
8. Okazaki, Y., Miyahara, K., Wade, N., and Hosoi, Y., "Effect of manganese and chromium on microstructure and toughness of Fe-Cr-Mn alloys resulting from solid-solution treatment", J. Japan. Inst. Metals, 1989, 53, 502.
9. Masumoto, H., Suemune, K., Nakajima, H., and Shimamoto, S., "Development of a high-strength high-manganese stainless steel for cryogenic use", Adv. Cryogenic Engng Mater., 1984, 30, 169.
10. Schiller, P., Review of materials selection for fusion reactors, J. Nucl. Mater., 1993, 206, 113.
11. Miyahara, K., Bae, D. S., Kimura, T., Shimoide, Y., and Hosoi, Y., "Strength properties and microstructure of high Mn-Cr austenitic steels as potential high temperature materials", ISIJ Int., 1996, 37, 878.
12. Hu, B., Kinoshita, H., Shibayama, T., and Takahashi, H., "Effect of helium on radiation behavior in low activation Fe-Cr-Mn alloys",

- Mater. Trans., 2002, 43, 622.
13. Harries, D. R., Butterworth, G. J., Hishinuma, A., and Wiffen, F. W., "Evaluation of reduced-activation options for fusion materials development", *J. Nucl. Mater.*, 1992, 191, 92.
 14. Kohyama, A., Grossbeck, M. L., and Piatti, G., "The application of austenitic stainless steels in advanced fusion systems: current limitations and future prospects", *J. Nucl. Mater.*, 1992, 191, 37.
 15. Shamardin, V. K., Bulanova, T. M., Golovanov, V. N., Neustroyev, V. S., Povstyanko, A. V., and Ostrovsky, Z. E., "Change in the properties of Fe-Cr-Ni and Fe-Cr-Mn austenitic steels under mixed and fast neutron irradiation", *J. Nucl. Mater.*, 1996, 233, 162.
 16. Onozuka, M., Saida, T., Hirai, S., Kusuhashi, M., Sato, I., and Hatakeyama, T., "Low-activation Mn-Cr austenitic stainless steel with further reduced content of long-lived radioactive elements", *J. Nucl. Mater.*, 1998, 255, 128.
 17. Klueh, R. L., Maziasz, P. J., and Lee, E. H., "Manganese as an Austenite Stabilizer in Fe-Cr-Mn-C Steels", *Mater. Sci. Eng. A*, 1988, 102, 115.
 18. Foldefiki, M., Ledbetter, H., and Uggowitzer, P., "Magnetic properties of Cr-Mn austenitic stainless steels", *J. Magnetism Magnet. Mater.*, 1992, 110, 185.
 19. Ruhi, G., Modi, O. P., and Singh, I. B., "Pitting of AISI 304L stainless steel coated with nano structured sol-gel alumina coatings in chloride containing acidic environments", *Corros. Sci.*, 2009, 51, 3057.
 20. Azumi, K., Ohtsuka, T., and Sata, N., "Mott-Schottky Plot of the Passive Film Formed on Iron in Neutral Borate and Phosphate Solutions", *J. Electrochem. Soc.*, 1987, 134, 1352.
 21. Macdonald, D. D., Ismail, K. M., and Sikora, E., "Characterization of the passive state on zinc", *J. Electrochem. Soc.*, 1998, 145, 3141.
 22. Qiao, Y. X., Zheng, Y. G., Ke, W., and Okafor, P. C., "Electrochemical behaviour of high nitrogen stainless steel in acidic solutions", *Corros. Sci.*, 2009, 51, 979.
 23. Yang, Y., Guo, L. J., and Liu, H., "Effect of fluoride ions on corrosion behavior of SS316L in simulated proton exchange membrane fuel cell (PEMFC) cathode environments", *J. Power Sources*. 2010, 195, 5651.
 24. Cheng, Y. F., Yang, C., and Luo, J. L., "Determination of the diffusivity of point defects in passive films on carbon steel", *Thin Solid Films*. 2002, 416, 169.
 25. Li, N., Li, Y., Wang, S., and Wang, F., "Electrochemical corrosion behavior of nanocrystallized bulk 304 stainless steel", *Electrochim. Acta*. 2006, 52, 760.
 26. Sato, N., "An overview of passivity of metals", *Corros. Sci.*, 1990, 31, 1.
 27. Ferreira, M. G. S., Hakiki, N. E., Goodlet, G., Faty, S., Simões, A. M. P., and Da Cunha Belo, M., "Influence of the temperature of film formation on the electronic structure of oxide films formed on 304 stainless steel", *Electrochim. Acta.*, 2001, 46, 3767.
 28. Oguzie, E. E., Li, J., Liu, Y., Chen, D., Li, Y., Yang, K., and Wang, F., "The effect of Cu addition on the electrochemical corrosion and passivation behavior of stainless steels", *Electrochim. Acta*, 2010, 55, 5028.
 29. Macdonald, D. D., "On the existence of our metals-based civilization I. Phase-space analysis", *Electrochim. Acta.*, 2010, 55, 5028.
 30. Macdonald, D. D. "On the existence of our metals-based civilization I. Phase-space analysis", *J. Electrochem. Soc.*, 2006, 153, B213.
 31. Fattah-alhosseini, A., and Farahani, H., "Electrochemical behaviour of AISI 304 stainless steel in sulfuric solution: Effects of acid concentration", *Iranian J. Mater. Sci. and Eng.*, 2013, 10, 31.
 32. Fattah-alhosseini, A., Soltani, F., Shirsalimi, F., Ezadi, B., and Attarzadeh, N., "The semiconducting properties of passive films formed on AISI 316 L and AISI 321 stainless steels: A test of the point defect model (PDM)", *Corros. Sci.*, 2011, 53, 3186.